

Particle Collisions and Negative Nonlocal Response of Ballistic Electrons

Andrey Shytov,¹ Jian Feng Kong,² Gregory Falkovich,^{3,4} and Leonid Levitov²

¹*School of Physics, University of Exeter, Stocker Road, Exeter EX4 4QL, United Kingdom*

²*Massachusetts Institute of Technology, Cambridge, Massachusetts 02139, USA*

³*Weizmann Institute of Science, Rehovot 76100, Israel*

⁴*Novosibirsk State University, Novosibirsk 630090, Russia*

 (Received 25 June 2018; published 26 October 2018)

An electric field that builds in the direction against current, known as negative nonlocal resistance, arises naturally in viscous flows and is thus often taken as a telltale of this regime. Here, we predict negative resistance for the ballistic regime, wherein the ee collision mean free path is greater than the length scale at which the system is being probed. Therefore, negative resistance alone does not provide strong evidence for the occurrence of the hydrodynamic regime; it must thus be demoted from the rank of irrefutable evidence to that of a mere forerunner. Furthermore, we find that negative response is log enhanced in the ballistic regime by the physics related to the seminal Dorfman-Cohen log divergence due to memory effects in the kinetics of dilute gases. The ballistic regime therefore offers a unique setting for exploring these interesting effects due to electron interactions.

DOI: [10.1103/PhysRevLett.121.176805](https://doi.org/10.1103/PhysRevLett.121.176805)

Electron interactions can alter transport characteristics of solids in a variety of interesting ways [1]. In particular, electron systems in which momentum-conserving ee collisions dominate transport are expected to exhibit collective hydrodynamic flows [2–5]. Viscous electron fluids can harbor interesting collective behaviors akin to those of classical fluids [6–15]. Manifestations of electron hydrodynamics, predicted theoretically, provide guidance to experiments that attempt to demonstrate this regime [16–18]. One such manifestation, discussed recently [14,16], is the “negative resistance” response, i.e., a current-induced electric field that builds in the direction against the applied current. In Ref. [14] negative resistance was predicted to arise naturally as the rate of momentum-conserving collisions exceeds the rate of momentum-relaxing collisions and the system transitions from the Ohmic regime to the hydrodynamic regime. In Ref. [16] its observation was used as a signature of the hydrodynamic regime, taking it for granted that negative resistance is a fingerprint of the hydrodynamic regime. However, so far the irrefutable status of this response has not been critically analyzed.

Here, we show that negative resistance can occur not only in the hydrodynamic regime, when the ee collision mean free path l_{ee} is the smallest length scale in the system, but also in the ballistic regime, when l_{ee} is much greater than the length scales at which the system is being probed. This behavior is illustrated in Fig. 1. As a result, negative resistance, taken alone, does not distinguish the hydrodynamic and ballistic regimes. Furthermore, the negative response value in the ballistic regime exceeds that in the hydrodynamic regime, which puts certain limitations on using this quantity as a diagnostic of hydrodynamics.

However, the two regimes can be distinguished by the temperature and carrier density dependence of the response. As discussed below, the response strength grows with temperature in the ballistic regime and decreases in the viscous regime. Likewise, it shows a different dependence on doping in the two regimes. These dependences, which are strikingly different in the two regimes, can provide guidance in delineating them in the existing [16,19–21] and future experiments. Negative resistance in the ballistic regime is supported by recent measurements in graphene and GaAs electron gases [20,21].

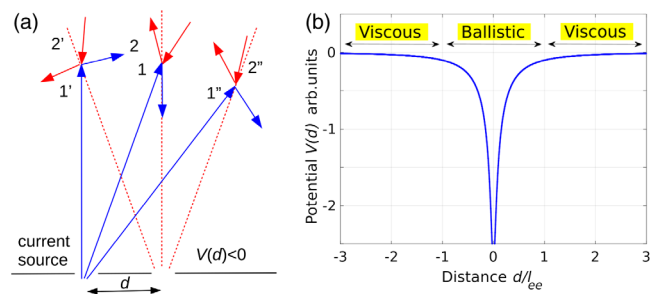


FIG. 1. Particles injected into an electron system from a current source (blue) undergo collisions with particles in the system bulk (red). The change in particle distribution is detected by a voltage probe at a distance d from the source, which measures particle flux into a contact at the boundary. The signal, dominated by ee interactions, is strongest at the distances smaller than the ee collision mean free path, $d \ll l_{ee}$. Panel (a) illustrates the mechanism of negative response: collisions between injected particles 1, 1', 1'' and background particles 2, 2', 2'' prevent some of the latter (2', 2'') from entering the probe. Panel (b) shows the predicted dependence of the probe potential vs. distance.

The origin of negative resistance can be understood most easily by considering transport in the half-plane geometry wherein particles are injected from a point source placed at the boundary as shown in Fig. 1(a). In this case there are two competing contributions to be considered. First, the injected particles, after colliding with the background particles, can be reflected into the voltage probe, which measures particle flux into the boundary. This produces a positive contribution to the measured voltage response. Second, the same collision processes also prevent some of the background particles from entering the probe, producing a negative contribution to the measured signal. Equivalently, this can be described as backscattering of a particle as a hole. We will see that the latter effect dominates, resulting in the net signal of a negative sign.

Interestingly, when the ee mean free path l_{ee} is greater than the distance between the source and the probe d , all the length scales $d < r < l_{ee}$ contribute equally to the response. That is, the negative response is dominated by particles making a large excursion at $r > d$ before returning to the probe as a hole. In this case we find the behavior

$$V(d) \sim -J_0 \gamma_{ee} \ln \frac{l_{ee}}{d}, \quad d \ll l_{ee} \quad (1)$$

where J_0 is the injected current and γ_{ee} is the ee collision rate. As a function of distance, the response grows as d decreases, diverging as $d/l_{ee} \rightarrow 0$. This dependence is illustrated in Fig. 1(b). In contrast, it falls off and becomes very small at large d , remaining negative in both the viscous regime $d \gg l_{ee}$ and the ballistic regime $d \ll l_{ee}$. As a function of distance to the probe, the negative response is

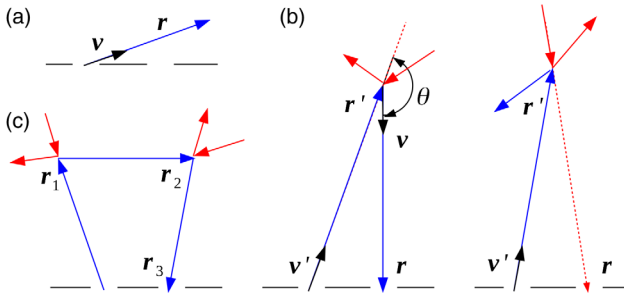


FIG. 2. Schematic illustration of different contributions to the nonlocal voltage response, arising in perturbation expansion of the solution of the transport equation, Eq. (4), in the ee collisions rate. Panels (a), (b), and (c), illustrate the first, second, and third terms, describing the result of $n = 0, 1$, and 2 collisions, respectively. The dominant contribution, which is of a negative sign, arises from the second contribution shown in (b), in which ambient carriers are scattered away and prevented from reaching the probe (see text). Such “ghost” processes produce negative flux into the probe. These processes are pictured in Fig. 1(a) (particles $1'$, $2'$ and $1''$, $2''$).

stronger in the ballistic regime than in the viscous regime. The log enhancement arises due to a large phase space of contributing trajectories, which make long excursions to the distances up to l_{ee} and then are scattered back to the probe as a hole, as illustrated in Figs. 1 and 2(b).

The origin and behavior of the negative response bears a similarity to the seminal memory effects due to multiple correlated collisions in kinetic theory, discovered by Dorfman and Cohen, and others [22,23]. This work made a surprising observation that virial expansion of the kinetic coefficients in gases breaks down due to multiple correlated collisions between two particles mediated by a third particle, which involve large excursions and log divergences similar to those found here. Manifestations of such memory effects, discussed so far, involved long-time power-law correlations in gases [24,25]. Here, instead of three correlated collisions, similar effects arise from a single collision, with the current source and voltage probe playing the role of two other collisions. One can therefore view the log enhancement in Eq. (1) as a direct manifestation of the memory effects predicted in kinetic theory.

Our transport problem can be readily analyzed with the help of the quantum kinetic equation

$$(\partial_t + \mathbf{v}\nabla - I_{ee})\delta f(\mathbf{r}, \mathbf{p}) = J_{\mathbf{r}, \mathbf{p}}, \quad J_{\mathbf{r}, \mathbf{p}} = J_0 \delta(\mathbf{r}). \quad (2)$$

Here, $\delta f(\mathbf{r}, \mathbf{p})$ describes particle distribution weakly perturbed near equilibrium. We assume $T \ll \epsilon_F$, in which case perturbed distribution is localized near the Fermi level and $\delta f(\mathbf{r}, \mathbf{p})$ can be parametrized as a function on the Fermi surface through the standard ansatz

$$\delta f(\mathbf{r}, \mathbf{p}) = -\frac{\partial f_0}{\partial \epsilon} \chi(\theta), \quad \chi(\theta) = \sum_m \chi_m e^{im\theta}, \quad (3)$$

with f_0 the equilibrium Fermi-Dirac distribution and θ the angle parametrizing the Fermi surface. Because of cylindrical symmetry, the ee collision operator is in general diagonal in the angular harmonics basis (see below). The quantity $J_{\mathbf{r}, \mathbf{p}}$ represents a current source placed at $\mathbf{r} = 0$. For conciseness, we ignore the angular anisotropy of the injected distribution.

The general solution of this equation is given by a formal perturbation expansion in the collision term

$$\delta f(\mathbf{r}, \mathbf{p}) = DJ_{\mathbf{r}, \mathbf{p}} + DI_{ee}DJ_{\mathbf{r}, \mathbf{p}} + DI_{ee}DI_{ee}DJ_{\mathbf{r}, \mathbf{p}} + \dots, \quad (4)$$

where $D = (\delta + \mathbf{v}\nabla)^{-1}$ is the Liouville propagator. Here, to describe a steady state, an infinitesimal positive δ was added in place of ∂_t to ensure that the steady-state response obeys causality. The collision processes described by this series are illustrated in Fig. 2. The first term represents particles moving freely away from the source:

$$\delta f_1(\mathbf{r}, \mathbf{p}) = \int_0^\infty dt \delta^{(2)}(\mathbf{r} - \mathbf{v}t) J_0, \quad (5)$$

where t is an auxiliary time parameter arising from solving transport equations as $\delta f_1 = \sum_{\mathbf{k}} e^{i\mathbf{k}\mathbf{r}} [J/(\delta + i\mathbf{k}\mathbf{v})] = \sum_{\mathbf{k}} \int_0^\infty dt e^{i\mathbf{k}(\mathbf{r}-\mathbf{v}t)} J$. The particles described by Eq. (5) never make it to the probe [Fig. 2(a)]. Other terms in Eq. (4) can also be evaluated in a similar manner. The second term describes injected particles scattered once by the background particles [Fig. 2(b)], giving

$$\delta f_2(\mathbf{r}, \mathbf{p}) = \sum_{\mathbf{r}', t, t'} \delta^{(2)}(\mathbf{r} - \mathbf{r}' - \mathbf{v}t) \sigma(\theta) \delta^{(2)}(\mathbf{r}' - \mathbf{v}'t') J_0, \quad (6)$$

where $\sum_{\mathbf{r}', t, t'}$ denotes $\int_0^\infty \int_0^\infty dt dt' \int d^2 r'$, and the ‘‘scattering cross section’’ σ describes the change of the distribution due to a scattering event. The cross section dependence vs. the angle between the incoming and outgoing velocities θ [see Fig. 2(b)] can be inferred from the form of the collision operator I_{ee} . For illustration, here we consider the simplest one-rate model of I_{ee} in which all nonconserved harmonics relax at equal rates [4,15],

$$I_{ee} \delta f = -\gamma_{ee} (\delta f - 2\hat{\mathbf{p}} \cdot \langle \hat{\mathbf{p}}' \delta f' \rangle_{\theta'} - \langle \delta f' \rangle_{\theta'}), \quad (7)$$

where the average $\langle \dots \rangle_{\theta'}$ is over \mathbf{p}' angles; δf and $\delta f'$ is a shorthand for $\delta f(\mathbf{p}, \mathbf{r})$ and $\delta f(\mathbf{p}', \mathbf{r})$, respectively. The last two terms in Eq. (7), which ensure momentum and particle number conservation, give the angle dependence

$$\sigma(\theta) = \gamma_{ee} (1 + 2 \cos \theta). \quad (8)$$

The two terms in this expression have very different meanings: the first, isotropic, term describes the addition of an incident particle after its velocity is randomized by collision, the second term describes momentum recoil of the background particles as a result of scattering.

Crucially, the cross section θ dependence in Eq. (8) is such that σ is positive at small θ but is *negative* in an interval of size $2\pi/3$ which includes the scattering angle $\theta = \pi$. The contribution of this process to the flux into the probe is dominated by the values $\theta \approx \pi - O(d/r)$. This contribution originates from scattering processes at relatively large distances from the injector $r \gg d$, giving a negative value which is log enhanced,

$$\delta V \sim J_0 \int_d^\infty \frac{d^2 r'}{r'^2} e^{-r'/l_{ee}} \sigma(\theta \approx \pi) \sim -J_0 \gamma_{ee} \ln \frac{l_{ee}}{d}. \quad (9)$$

The log factor is large in the ballistic regime $l_{ee} \gg d$.

The textbook estimate $\gamma_{ee} \sim bR^* T^2 / \epsilon_F^2$, where R^* is the effective Rydberg constant near ϵ_F and b is a numerical factor of order unity, indicates that the response grows with temperature (T) and decreases with carrier density (n). This is in contrast to the negative response in the hydrodynamic

regime, which is proportional to viscosity and thus scales inversely with γ_{ee} [14]. The opposite signs of the dependence vs. T and n may help distinguish the ballistic and viscous negative response.

Higher-order terms in Eq. (4) describe multiple scattering. For example, the third term gives a contribution to particle flux into the probe of the form [Fig. 2(c)]

$$J_0 \gamma_{ee}^2 \int \int \frac{d^2 r_1 d^2 r_2 e^{-L/l_{ee}}}{|\mathbf{r}_1| |\mathbf{r}_2 - \mathbf{r}_1| |\mathbf{r}_3 - \mathbf{r}_2|} \sim \gamma_{ee} J_0, \quad (10)$$

where $L = |\mathbf{r}_1| + |\mathbf{r}_2 - \mathbf{r}_1| + |\mathbf{r}_3 - \mathbf{r}_2|$. This contribution is nondivergent in the limit of a proximal probe $d \ll l_{ee}$, and thus is subleading to the second term by a log factor.

By a similar dimensional argument one can show that the n th order terms give the contributions

$$J_0 \gamma_{ee}^n \int \dots \int \frac{d^2 r_1 d^2 r_2 \dots d^2 r_n}{|\mathbf{r}_1| |\mathbf{r}_1 - \mathbf{r}_2| \dots |\mathbf{r}_n - \mathbf{r}_{n-1}|} \sim \gamma_{ee}^n \frac{l_{ee}^{2n}}{l_{ee}^{n+1}} \sim \gamma_{ee}. \quad (11)$$

This behavior of higher-order terms, featuring identical scaling with γ_{ee} , simply means that perturbation expansion is ill defined and cannot be used to evaluate the response outside the ballistic regime. As noted above, the log divergence of the second term and the power-law divergence of higher-order terms are related to the seminal divergences found in the breakdown of the virial expansion in kinetic theory due to memory effects in multiple correlated collisions [22,23].

We now proceed to show that the nonlocal resistance also remains negative outside the ballistic regime, that is at large distances $r \gg l_{ee}$. To describe this regime we need to incorporate boundary scattering into the model. Momentum relaxation at the boundary is usually described by diffuse boundary conditions, leading to a cumbersome mathematical boundary value problem. Instead, to simplify the analysis, here we extend particle dynamics from the halfplane to the full plane, and model momentum relaxation on the line $y = 0$ through adding an additional term to the collision operator as

$$I_{ee} \rightarrow I_{ee} + I_{bd}, \quad I_{bd} \delta f = -\alpha \delta(y) P' \delta f. \quad (12)$$

Here, P' is a projection on the harmonics $m = \pm 1$: $P' \delta f = 2\hat{\mathbf{p}} \cdot \langle \hat{\mathbf{p}}' \delta f(\mathbf{p}') \rangle_{\mathbf{p}'}$. The limit $\alpha \rightarrow \infty$ is expected to mimic the no-slip boundary conditions. Carrier distribution induced by an injector is described by

$$[\mathbf{v}\nabla - I_{ee} + \alpha(\mathbf{r})P'] \delta f(\mathbf{r}, \mathbf{p}) = J_0 \delta(\mathbf{r}). \quad (13)$$

The solution of this transport problem can be obtained in Fourier representation $\delta f(\mathbf{r}, \mathbf{p}) = \sum_{\mathbf{k}} e^{i\mathbf{k}\mathbf{r}} \delta f_{\mathbf{k}}(\mathbf{r})$:

$$(i\mathbf{k}\mathbf{v} - I_{ee} + \hat{\alpha}P')\delta f_{\mathbf{k}}(\mathbf{r}) = J_0, \quad \langle \mathbf{k} | \hat{\alpha} | \mathbf{k}' \rangle = \alpha \delta_{k_1 - k'_1}, \quad (14)$$

where the delta function $\delta_{k_1 - k'_1}$ reflects translational invariance of the line $y = 0$ in the x direction.

Next, we transform to the angular harmonics basis (3). We formally solve Eq. (14) by a perturbation series in α :

$$|\delta f\rangle = (G - G\hat{\alpha}G + G\hat{\alpha}G\hat{\alpha}G - \dots)|0\rangle J_0, \quad (15)$$

where, $G = 1/(i\mathbf{k}\mathbf{v} - I_{ee})$ is the free-space Green's function, $|0\rangle$ denotes the $m = 0$ angular harmonic. For conciseness, we absorb P' into $\hat{\alpha}$ and suppress the $\partial f_0/\partial \epsilon$ factor. The first term represents a solution of Eq. (14) for a point source in free space and no momentum relaxation, $\alpha = 0$. Other terms describe scattering at the line $y = 0$. Because of P' projection, every encounter with the line generates a contribution of the form $e^{i\theta} + e^{-i\theta} = 2\cos\theta$. We can therefore replace Eq. (15) by an equivalent free-space problem with a line source proportional to current density at the boundary:

$$[ikv \cos(\theta - \theta_k) - I_{ee}]|\delta f\rangle = J_0(1 + w_{k_1} 2\cos\theta). \quad (16)$$

Here, θ is the velocity angle and θ_k is the vector \mathbf{k} angle, $k_1 + ik_2 = ke^{i\theta_k}$. The first term 1 represents the original point source at $\mathbf{r} = 0$; the terms $w_{k_1} e^{\pm i\theta}$ represent a source distributed on the $y = 0$ line (no k_2 dependence). The weights w_{k_1} are evaluated in the Supplemental Material [26].

In the basis (3), the transport problem (16) is represented as a system of coupled equations

$$\frac{ikv}{2}(e^{i\theta_k}\chi_{m+1} + e^{-i\theta_k}\chi_{m-1}) + \gamma_m\chi_m = J_m, \quad (17)$$

where γ_m are the eigenvalues of the operator I_{ee} , which is diagonal in the basis (3), and J_m take values J_0 and $w_{k_1}J_0$ for $m = 0, \pm 1$ and zero otherwise. Here, we used the identity $\cos(\theta - \theta_k) = (1/2)(e^{i(\theta - \theta_k)} + e^{-i(\theta - \theta_k)})$, interpreting the factors $e^{\pm i\theta}$ as shift operators $m \rightarrow m \mp 1$.

In our one-rate model the eigenvalues of I_{ee} are $\gamma_m = \gamma_{ee}$ for $|m| > 1$, and zero otherwise. We will now show that in this case the coupled equations, Eq. (17), have a solution with the m dependence of an exponential form

$$\chi_m = e^{-im\theta_k} \times \begin{cases} c_1(-iz)^{m-1}, & m > 0, \\ c_0, & m = 0, \\ c_{-1}(-iz)^{-(m+1)}, & m < 0, \end{cases} \quad (18)$$

with $|z| < 1$. Plugging it into Eq. (17) with any $m \neq 0, \pm 1$ gives an algebraic equation $(vk/2)(z - z^{-1}) + \gamma_{ee} = 0$. This equation is solved by

$$z = e^{-\lambda}, \quad \sinh \lambda = \frac{\gamma_{ee}}{kv}. \quad (19)$$

The $m = \pm 1$ and $m = 0$ equations are

$$c_0 - izc_{\pm 1} = e^{\pm i\theta_k} w_{k_1} \frac{2J_0}{ikv}, \quad c_1 + c_{-1} = \frac{2J_0}{ikv}. \quad (20)$$

These equations give values

$$c_0 = J_0 \frac{2w_{k_1} \cos\theta_k + iz}{ikv}, \quad c_{\pm 1} = J_0 \frac{z \mp 2w_{k_1} \sin\theta_k}{ikvz}. \quad (21)$$

The full distribution can now be evaluated by carrying out the sum over m . This gives a closed-form expression

$$\delta f_{\mathbf{k}}(\theta) = c_0 + \frac{c_1 e^{i(\theta - \theta_k)}}{1 + iz e^{i(\theta - \theta_k)}} + \frac{c_{-1} e^{-i(\theta - \theta_k)}}{1 + iz e^{-i(\theta - \theta_k)}}, \quad (22)$$

where the three terms represent the contributions of the harmonics $m = 0$, $m > 0$, and $m < 0$, respectively.

We model the voltage probe as a small slit which measures the incoming particle flux F (see Fig. 1):

$$V(d) = \frac{e\omega}{G} F, \quad F = \int_{-\pi}^0 \frac{d\theta}{2\pi} Dv \sin\theta \chi(r, \theta), \quad (23)$$

where the integration limits $-\pi < \theta < 0$ select particles which are incident on the boundary. Here, w is the slit width, e is electron charge, $G = (4e^2/h)(2w/\lambda_F)$ is the slit conductance, and D is the density of states. Particles incident at an angle θ contribute to the flux with the weight $v \sin\theta$. The voltage $V(d)$ does not depend on the slit width w , as expected.

We emphasize that the voltage probe measures the incoming current flux rather than the current-induced potential or charge density change. Indeed, the injected current gives rise to a space charge buildup in the system bulk. This space charge, due to quasineutrality, shifts local chemical potential. However, in a steady state, a change in the local chemical potential does not lead to a net current into the boundary and therefore does not contribute to the voltage signal measured by the probe.

We evaluate voltage on the probe, Eq. (23), using the carrier distribution (22), Fourier transformed to real space. The flux for the distribution (22) can be analyzed by summing the contributions of different harmonics with the help of the identity

$$\int_{-\pi}^0 \frac{d\theta}{2\pi} v \sin\theta e^{im\theta} = \begin{cases} \frac{v}{\pi(m^2 - 1)}, & m \text{ even}, \\ \pm \frac{iv}{4}, & m \text{ odd}, m = \pm 1, \\ 0, & m \text{ odd}, m \neq \pm 1. \end{cases} \quad (24)$$

The resulting response, illustrated in Fig. 1(b), is negative in both the ballistic and viscous regimes. It is more negative in the ballistic regime, $d \ll l_{ee}$, than in the viscous regime, $d \gg l_{ee}$. Therefore, the sign of the response does not distinguish between the two regimes. However, since in the ballistic regime the response scales as γ_{ee} , whereas in

the viscous regime it scales as γ_{ee}^{-1} , the T and n dependences will be of opposite signs in the two cases, providing a clear signature that may help distinguish the two regimes.

For monolayer graphene the negative response of ballistic electrons, derived above, is proportional to $\lambda_F \gamma_{ee} \sim T^2/n$, decreasing with n and growing with T . Yet, for a viscous flow the response is proportional to η/n^2 , where η is dynamic viscosity. The estimate $\eta = nmv_F l_{ee}/4$ then predicts a density-independent response. Interestingly, the response reported in Ref. [16] decreases with n and grows with T at not-too-high temperatures, resembling the behavior expected for ballistic electrons. The vicinity resistance geometry [20] therefore provides an ideal setting in which the effects of ee interactions in the ballistic regime can be explored.

Part of this work was performed at the Aspen Center for Physics, which is supported by National Science Foundation Grant No. PHY-1607611. We acknowledge support by A*STAR NSS (PhD) Fellowship (J. F. K.); the Minerva Foundation, ISF Grant 882, the RSF Project No. 14-22-00259 (G. F.); the Center of Integrated Quantum Materials under NSF Grant No. DMR-1231319; the MIT Center for Excitonics, the Energy Frontier Research Center funded by the U.S. Department of Energy, Office of Science under Award No. DE-SC0001088, and Army Research Office Grant No. W911NF-18-1-0116 (L. L.).

[1] E. M. Lifshitz and L. P. Pitaevskii, *Physical Kinetics* (Pergamon Press, New York, 1981).
 [2] K. Damle and S. Sachdev, Nonzero-temperature transport near quantum critical points, *Phys. Rev. B* **56**, 8714 (1997).
 [3] R. N. Gurzhi, Hydrodynamic effects in solids at low temperature, *Usp. Fiz. Nauk* **94**, 689 (1968).
 [4] M. J. M. de Jong and L. W. Molenkamp, Hydrodynamic electron flow in high-mobility wires, *Phys. Rev. B* **51**, 13389 (1995).
 [5] R. Jaggi, Electron-fluid model for the dc size effect, *J. Appl. Phys.* **69**, 816 (1991).
 [6] M. Müller, J. Schmalian, and L. Fritz, Graphene: A Nearly Perfect Fluid, *Phys. Rev. Lett.* **103**, 025301 (2009).
 [7] A. V. Andreev, S. A. Kivelson, and B. Spivak, Hydrodynamic Description of Transport in Strongly Correlated Electron Systems, *Phys. Rev. Lett.* **106**, 256804 (2011).
 [8] D. Forcella, J. Zaanen, D. Valentinis, and D. van der Marel, Electromagnetic properties of viscous charged fluids, *Phys. Rev. B* **90**, 035143 (2014).

[9] A. Tomadin, G. Vignale, and M. Polini, Corbino Disk Viscometer for 2D Quantum Electron Liquids, *Phys. Rev. Lett.* **113**, 235901 (2014).
 [10] D. E. Sheehy and J. Schmalian, Quantum Critical Scaling in Graphene, *Phys. Rev. Lett.* **99**, 226803 (2007).
 [11] L. Fritz, J. Schmalian, M. Müller, and S. Sachdev, Quantum critical transport in clean graphene, *Phys. Rev. B* **78**, 085416 (2008).
 [12] B. N. Narozhny, I. V. Gornyi, M. Titov, M. Schütt, and A. D. Mirlin, Hydrodynamics in graphene: Linear-response transport, *Phys. Rev. B* **91**, 035414 (2015).
 [13] A. Cortijo, Y. Ferreirós, K. Landsteiner, and M. A. H. Vozmediano, Hall Viscosity from Elastic Gauge Fields in Dirac Crystals, *Phys. Rev. Lett.* **115**, 177202 (2015).
 [14] L. Levitov and G. Falkovich, Electron viscosity, current vortices and negative nonlocal resistance in graphene, *Nat. Phys.* **12**, 672 (2016).
 [15] H. Guo, E. Ilseven, G. Falkovich, and L. Levitov, Higher-than-ballistic conduction of viscous electron flows, *Proc. Natl. Acad. Sci. U.S.A.* **114**, 3068 (2017).
 [16] D. A. Bandurin *et al.*, Negative local resistance caused by viscous electron backflow in graphene, *Science* **351**, 1055 (2016).
 [17] J. Crossno *et al.*, Observation of the Dirac fluid and the breakdown of the Wiedemann-Franz law in graphene, *Science* **351**, 1058 (2016).
 [18] P. J. W. Moll, P. Kushwaha, N. Nandi, B. Schmidt, and A. P. Mackenzie, Evidence for hydrodynamic electron flow in PdCoO₂, *Science* **351**, 1061 (2016).
 [19] A. I. Berdyugin *et al.*, Measuring Hall viscosity of graphene's electron fluid, [arXiv:1806.01606](https://arxiv.org/abs/1806.01606).
 [20] D. A. Bandurin *et al.*, Fluidity onset in graphene, [arXiv:1806.03231](https://arxiv.org/abs/1806.03231).
 [21] B. A. Braem *et al.*, Scanning Gate Microscopy in a Viscous Electron Fluid, [arXiv:1807.03177](https://arxiv.org/abs/1807.03177).
 [22] J. R. Dorfman and E. G. D. Cohen, On the density expansion of the pair distribution function for a dense gas not in equilibrium, *Phys. Lett.* **66**, 124 (1965).
 [23] R. Peierls, *Surprises in Theoretical Physics*, Princeton Series in Physics (Princeton University Press, Princeton, NJ, 1979).
 [24] J. R. Dorfman and E. G. D. Cohen, Velocity Correlation Functions in Two and Three Dimensions, *Phys. Rev. Lett.* **25**, 1257 (1970).
 [25] A. Dmitriev, M. Dyakonov, and R. Jullien, Non-Boltzmann classical correction to the velocity auto-correlation function for isotropic scattering in two dimensions, *Phys. Rev. B* **71**, 155333 (2005).
 [26] See Supplemental Material at <http://link.aps.org/supplemental/10.1103/PhysRevLett.121.176805> for a derivation of the boundary currents, representing sources in Eq. (16), by the method of quasi-hydrodynamic variables.